



Supplementary Materials: Absorption and Emission Spectroscopic Investigation of Thermal Dynamics and Photo-Dynamics of the Rhodopsin Domain of the Rhodopsin-Guanylyl Cyclase from the Nematophagous Fungus *Catenaria anguillulae*

Alfons Penzkofer, Ulrike Scheib, Katja Stehfest and Peter Hegemann

S1. Amino Acid Sequence

The amino acid sequence of the here investigated recombinant synthesized rhodopsin CaRh is displayed in Figure S1. It was added MS at the N-terminus and ENLYFQGVDHHHHHH at the C-terminus to the Rh domain of the full-length CaRhGC protein. Its apoprotein molar mass is $M_{pr} = 45484.94 \text{ g mol}^{-1}$. It contains 14 Tyr, 12 Trp, and 26 Phe residues.

```
10      20      30      40      50      60
MSMKDKDNNL RGACSGCSCP EYCYSPTSTL CDDCKCSVTK HPIVEQPLTR NGSFRSSGAS
70      80      90     100     110     120
LLPSPSQPNI KVTGSSTASS NANMRNRQNN SLSVSNVRST SSASSSNVSS PANSRPGSPS
130     140     150     160     170     180
KQSALQQYQT NIADMWSWDM MLSTPSLKFL TGQFIMWAIL TVAGAFYALF IQERQAYNRG
190     200     210     220     230     240
WADIWYGYGA FGFGIGIAFS YMGFAGARNP EKKALSLCLL GVNIIAFSSY ILIMLRLTPT
250     260     270     280     290     300
IEGTLSPVE PARYLEWIAT CPVLILLISE ITQADHNAWG VVFSDYALVV CGFFGAVLPP
310     320     330     340     350     360
YPWGNLFNIL SCAFFSFVVY SLWRSFTGAI NGETPCNIEV NGLRWTRFST VTTWTLFPLS
370     380     390     400     410
WFAFTSGMLS FTMTEASFMT IDIGAKVFLT LVLVNSTVEN LYFQGVDHHH HHH
```

Figure S1. Amino acid sequence of CaRh

S2. Absorption Cross-Section Determination

The absorption cross-section spectrum shape $\sigma_{a, \text{CaRh}}(\lambda)$ of CaRh (solid curve in top part of Figure S2) is equal to the absorption coefficient shape $\alpha_a(\lambda)$ of Figure 1. The absolute absorption cross-section spectrum $\sigma_{a, \text{CaRh}}(\lambda)$ of CaRh is determined by setting the absorption cross-section of CaRh at $\lambda = 270 \text{ nm}$ equal to the apoprotein Trp, Tyr, and Phe absorption cross-section contribution $\sigma_{26F+14Y+12W}(270 \text{ nm})$ and some estimated retinal absorption cross-section contribution [S1]. The involved absorption cross-section spectra of Phe, Tyr, and Trp were taken from [13]. The apoprotein

absorption cross-section spectrum $\sigma_{26F+14Y+12W}$ of CaRh is shown by the dashed curve in the top part of Figure S2. It was calculated as the sum of the absorption cross-section spectra of 26 Phe, 14 Tyr, and 12 Trp residues present in one apoprotein. The CaRh molecule number density was determined by

$$N_{CaRh} = \frac{\alpha_{a,apo}(270\text{ nm})}{\sigma_{26F+14Y+12W}(270\text{ nm})} = \frac{\alpha_{a,CaRh}(270\text{ nm}) - \alpha_{a,retinal}(270\text{ nm})}{\sigma_{26F+14Y+12W}(270\text{ nm})}, \quad (S1)$$

and the absorption cross-section spectrum of CaRh was set to

$$\sigma_{a,CaRh}(\lambda) = \frac{\alpha_{a,CaRh}(\lambda)}{N_{CaRh}}. \quad (S2)$$

The values used in the calculations were $\alpha_{a,CaRh}(270\text{ nm}) = 17.22\text{ cm}^{-1}$, $\alpha_{a,retinal}(270\text{ nm}) = 1.8\text{ cm}^{-1}$, and $\sigma_{26F+14Y+12W}(270\text{ nm}) = 3.08 \times 10^{-16}\text{ cm}^2$ giving $N_{CaRh} = 5.01 \times 10^{16}\text{ cm}^{-3}$.

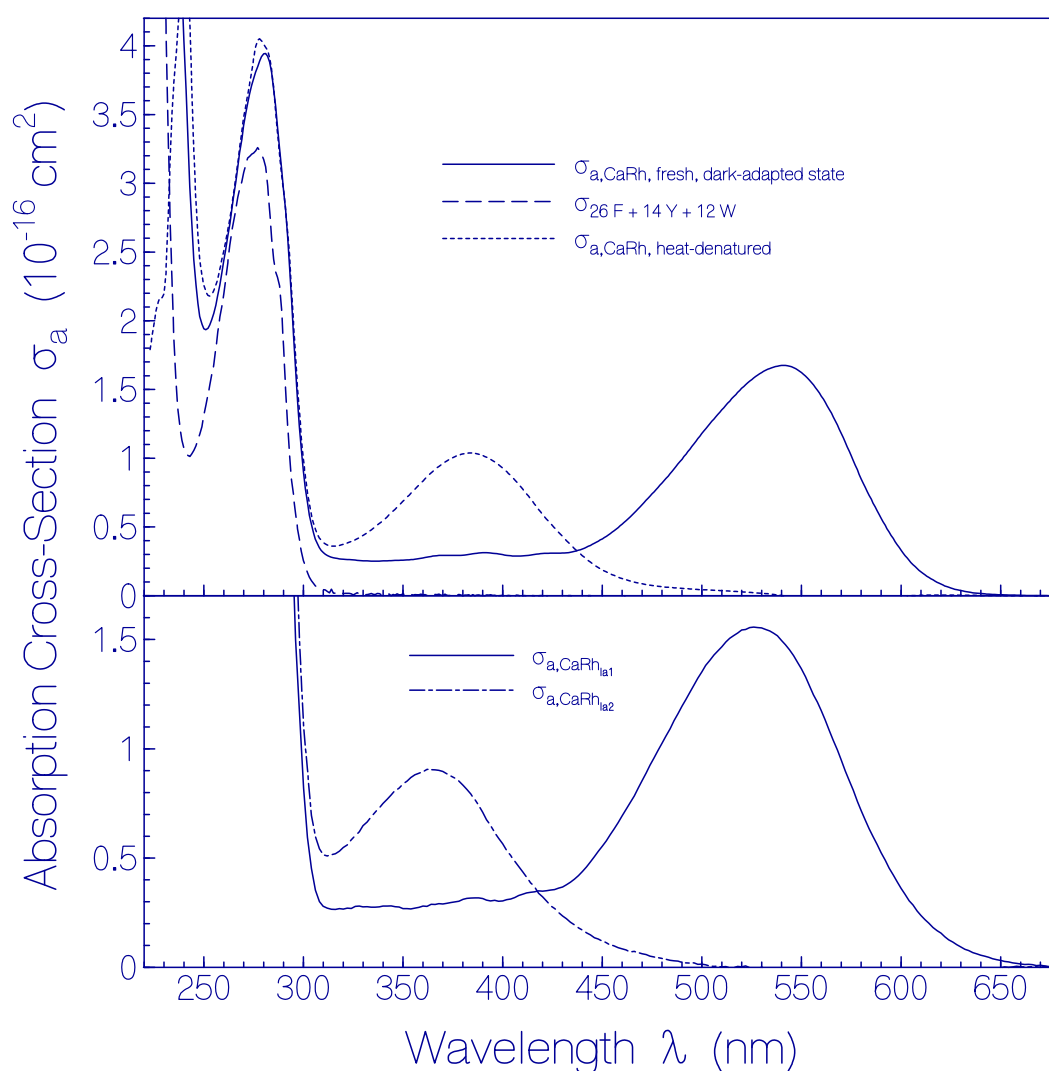


Figure S2. Absorption cross-section spectra. Curves are identified by the legends.

The absorption cross-section spectrum $\sigma_{a,CaRh, \text{fresh, dark-adapted state}}(\lambda > 310\text{ nm})$ is the absorption cross-section spectrum of PRSB in CaRh for $\lambda > 310\text{ nm}$. The determination of $\sigma_{a,CaRh, \text{heat-denatured}}$ is described in section 2.2.1 of the main text. The main band with absorption maximum at 384 nm is

the S₀-S₁ absorption cross-section band of RSB in heat-denatured CaRh. The absorption cross-section spectrum $\sigma_{a, CaRh_{la1}}(\lambda)$ is the absorption cross-section spectrum of CaRh in its light-adapted ground-state la1 (G_{la1}). Its determination is described in section S7. $\sigma_{a, CaRh_{la1}}(\lambda > 310 \text{ nm})$ is caused by the excitation of PRSB_{all-trans, la1}. The absorption cross-section spectrum $\sigma_{a, CaRh_{la2}}(\lambda)$ is the absorption cross-section spectrum of CaRh in its light-adapted state la2 (CaRh_{la2}). Its determination is described in section S7. The main band with absorption maximum at 365 nm is the S₀-S₁ absorption cross-section band of RSB_{13-cis} in CaRh_{la2}.

S3. Nano-Cluster Size of a Fresh Centrifuged CaRh Sample

The nano-cluster size of fresh CaRh is determined analogous to the description in [6] and [S2]. The scattering cross-section σ_s is obtained from the scattering coefficient α_s by $\sigma_s = \alpha_s / N_{CaRh}$. For the sample used in Figure 1, at $\lambda = 632.8 \text{ nm}$ it is $\alpha_s(\lambda) = \alpha_s(\lambda_0)(\lambda_0 / \lambda)^\gamma = 0.0702 \text{ cm}^{-1}$ ($\lambda_0 = 800 \text{ nm}$, $\alpha_s(\lambda_0) = 0.046 \text{ cm}^{-1}$, $\gamma = 1.8$) and $\sigma_s(\lambda) = 1.40 \times 10^{-18} \text{ cm}^2$ ($N_{CaRh} = 5.01 \times 10^{16} \text{ cm}^{-3}$).

The scattering cross-section σ_s is theoretically given by [7]

$$\sigma_s = M_{sca} \sigma_{R,m} = \beta_m \tilde{M} \sigma_{R,m} \quad (S3)$$

where $M_{sca} = \beta_m \tilde{M}$ is the aggregation scattering enhancement factor, β_m is the degree of aggregation (average number of protein molecules per cluster particle), \tilde{M} is the total Mie scattering function ($\tilde{M} \leq 1$ decreasing with increasing aggregate size [7]), and $\sigma_{R,m}$ is the monomer Rayleigh scattering cross-section. The monomer Rayleigh scattering cross-section is given by [7]

$$\sigma_{R,m}(\lambda) = \frac{8\pi}{3} \frac{4\pi^2 n_s^4}{\lambda^3} V_m^2 \left(\frac{n_{pr}^2 - n_s^2}{n_{pr}^2 + 2n_s^2} \right)^2 = \frac{8\pi}{3} \frac{4\pi^2 n_s^4}{\lambda^3} \left(\frac{M_{pr}}{N_A \rho_{pr}} \right)^2 \left(\frac{n_{pr}^2 - n_s^2}{n_{pr}^2 + 2n_s^2} \right)^2. \quad (S4)$$

Thereby n_s is the refractive index of the solvent (water buffer) at wavelength λ , n_{pr} is the refractive index of the protein at wavelength λ , $V_m = M_{pr} / (N_A \rho_{pr})$ is the volume of one protein molecule, M_{pr} is the molar mass of the protein monomer ($M_{pr} = 45484.94 \text{ g mol}^{-1}$ for CaRh apoprotein), $N_A = 6.022142 \times 10^{23} \text{ mol}^{-1}$ is the Avogadro constant, and ρ_{pr} is the mass density of the protein (typical value for proteins is $\rho_{pr} \approx 1.412 \text{ g cm}^{-3}$ [S3]). These numbers give a protein monomer volume of $V_m \approx 53.49 \text{ nm}^3$ and a protein monomer radius of $a_m = [3V_m / (4\pi)]^{1/3} \approx 2.34 \text{ nm}$. At $\lambda = 632.8 \text{ nm}$ there is $n_s = 1.332$ and $n_{pr} \approx 1.589$ [S4] giving $\sigma_{R,m}(632.8 \text{ nm}) = 2.838 \times 10^{-21} \text{ cm}^2$. Insertion into Equation (S3) gives $M_{sca} = \beta_m \tilde{M} = \sigma_s / \sigma_{R,m} \approx 494$. The small value of $\gamma = 1.8$ indicates a small \tilde{M} and a large cluster volume $V_{ag} = \beta_m V_m / \kappa_{f,m}$ with small volume fill factor $\kappa_{f,m}$ [7].

S4. Fluorescence Quantum Distribution of Heat-Denatured CaRh

The fluorescence quantum distribution of the heat-denatured CaRh sample of Figure 4 is shown in Figure S3. The corresponding attenuation coefficient spectrum is shown by the thick solid curve in Figure 4a (4 °C, end). Fluorescence excitation occurred at $\lambda_{F,exc} = 360$ nm.

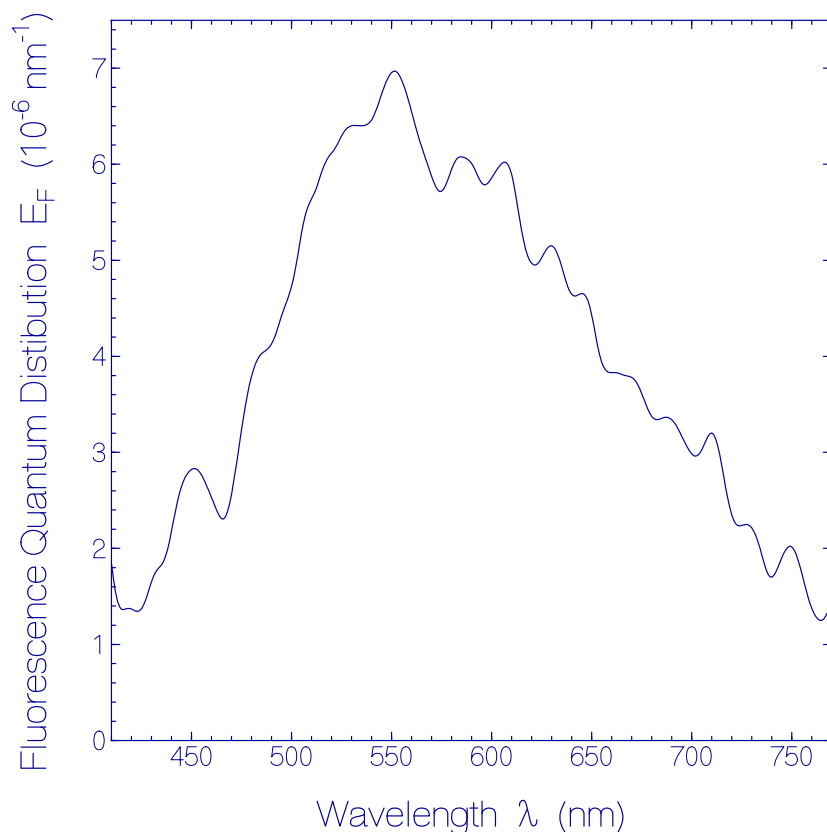


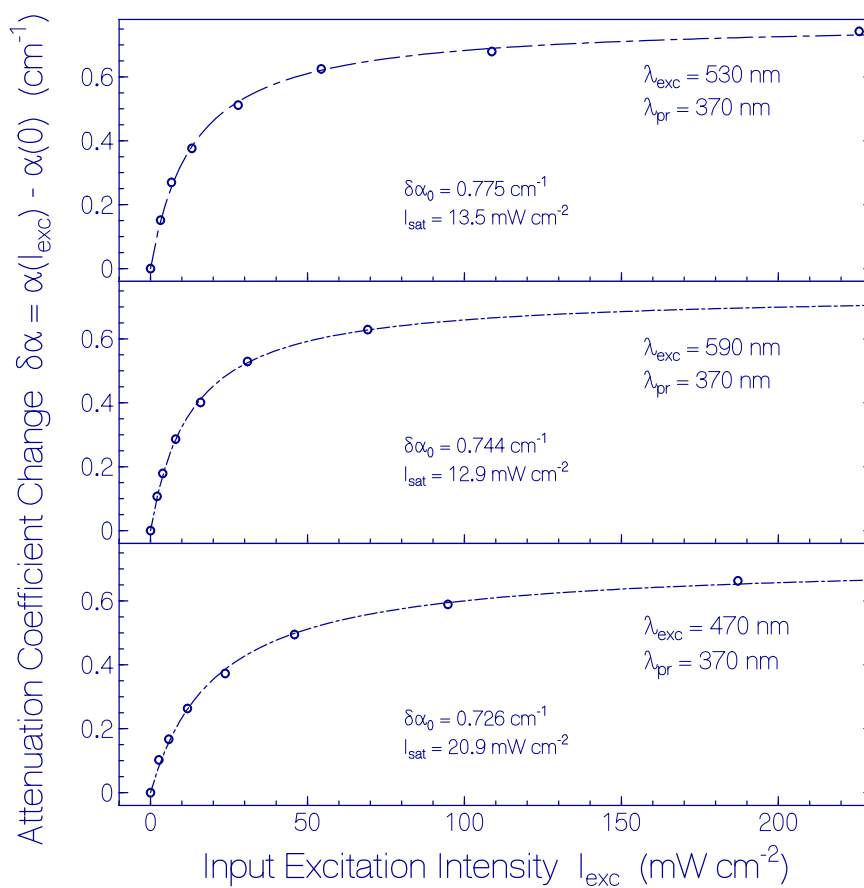
Figure S3. Fluorescence quantum distribution of heat-denatured CaRh in pH 7.3 HEPES/MOPS buffer for fluorescence excitation wavelength $\lambda_{F,exc} = 360$ nm (excitation of RSB, belongs to thick solid curve of attenuation coefficient spectrum shown in Figure 4a).

S5. Excitation intensity dependent steady-state attenuation coefficient changes

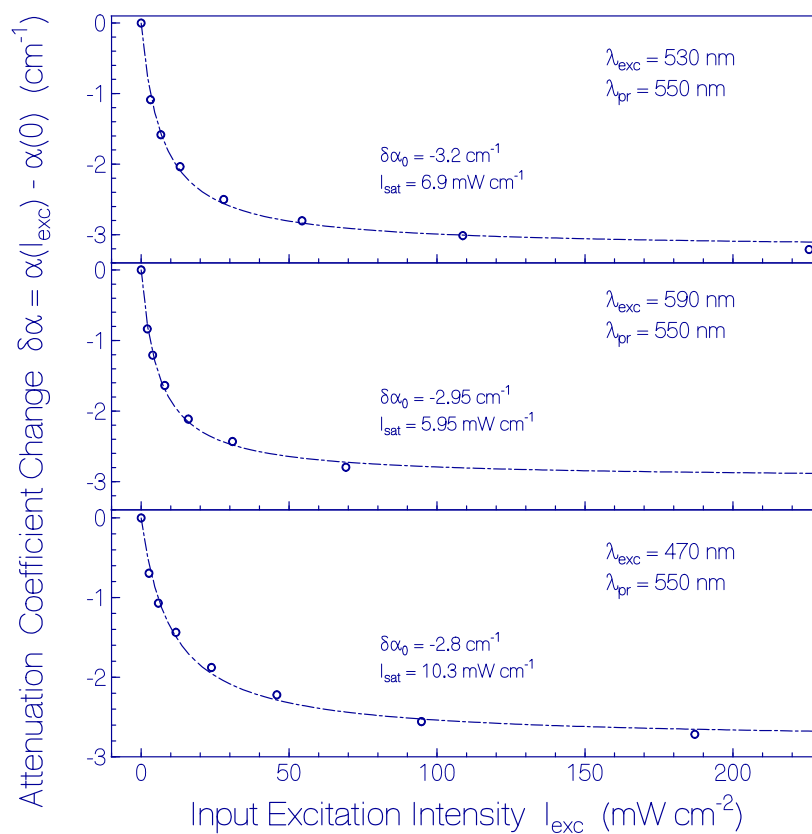
The attenuation coefficient change $\delta\alpha(\lambda_{pr}, \lambda_{exc}, I_{exc}) = \alpha_{\text{extremum}}(\lambda_{pr}, \lambda_{exc}, I_{exc}) - \alpha(\lambda_{pr}, I_{exc} = 0)$ versus excitation intensity for the excitation wavelengths $\lambda_{exc} = 530$ nm (LED 530 nm), 590 nm (LED 590 nm) and 470 nm (LED 470 nm) is shown in Figure S4a for $\lambda_{pr} = 370$ nm and in Figure S4b for $\lambda_{pr} = 550$ nm. The circles are experimental data. The curves are nonlinear regression fits to the experimental data using the relation [S5]

$$\delta\alpha(\lambda_{pr}, \lambda_{exc}, I_{exc}) = \delta\alpha_0(\lambda_{pr}) \frac{I_{exc} / I_{sat}(\lambda_{exc}, \lambda_{pr})}{1 + I_{exc} / I_{sat}(\lambda_{exc}, \lambda_{pr})}, \quad (S5)$$

with $\delta\alpha_0$ and $I_{sat}(\lambda_{exc}, \lambda_{pr})$ listed in the sub-figures. The saturation intensity is inverse proportional to absorption cross-section $\sigma_a(\lambda_{exc})$ and the absorption recovery time τ_{rec} [S5].



(a)



(b)

Figure S4. Dependence of attenuation coefficient change $\delta\alpha(\lambda_{pr}, \lambda_{exc}, I_{exc}) = \alpha_{\text{extremum}}(\lambda_{pr}, \lambda_{exc}, I_{exc}) - \alpha(\lambda_{pr}, I_{exc} = 0)$ of CaRh in pH 7.3 HEPES/MOPS buffer (a) at $\lambda_{pr} = 370$ nm and (b) at $\lambda_{pr} = 550$ nm on excitation light intensity I_{exc} for $\lambda_{exc} = 530$ nm (top part), 590 nm (middle part), and 470 nm (bottom part). Circles are experimental data. The curves are nonlinear regression fits to the experimental data using the relation $\delta\alpha(\lambda_{pr}, I_{exc}) = \delta\alpha_0(I_{exc}/I_{sat})/(1 + I_{exc}/I_{sat})$ with $\delta\alpha_0$ and I_{sat} listed in the sub-figures.

S6. Calculation of quantum yield of photo-degradation

The quantum yield of photodegradation ϕ_d is given by

$$\phi_d = \frac{\Delta N_{da}}{\Delta n_{ph,abs}} \quad (S6)$$

where ΔN_{da} is the increment of length-integrated number density of degraded dark-adapted CaRh (Rh-541) and $\Delta n_{ph,abs}$ is the increment of absorbed excitation photons by light-adapted CaRh (Rh-527).

ΔN_{da} is given by

$$\Delta N_{da} = \bar{N}_{da} l_{exc} \frac{\Delta\alpha_a(\lambda_{pr})}{\bar{\alpha}_a(\lambda_{pr})} = \frac{\bar{\alpha}_a(\lambda_{pr})}{\sigma_{a,da}(\lambda_{pr})} l_{exc} \frac{\Delta\alpha_a(\lambda_{pr})}{\bar{\alpha}_a(\lambda_{pr})} = l_{exc} \frac{\Delta\alpha_a(\lambda_{pr})}{\sigma_{a,da}(\lambda_{pr})} \quad (S7)$$

$\bar{N}_{da} = \bar{\alpha}_a(\lambda_{pr}) / \sigma_{a,da}(\lambda_{pr})$ is the average number density of CaRh in the dark-adapted state.

$\bar{\alpha}_a(\lambda_{pr}) = [\alpha_{a, \text{begin of exposure interval}}(\lambda_{pr}) + \alpha_{a, \text{recovered after end of exposure interval}}(\lambda_{pr})] / 2$ is the average absorption coefficient of dark-adapted CaRh at λ_{pr} (here used $\lambda_{pr} = \lambda_{da,max} = 541$ nm). l_{exc} is the sample length in excitation direction, $\Delta\alpha_a(\lambda_{pr}) = \alpha_{a, \text{begin of exposure interval}}(\lambda_{pr}) - \alpha_{a, \text{recovered after end of exposure interval}}(\lambda_{pr})$ is the absorption coefficient change of dark-adapted CaRh at the probe wavelength λ_{pr} due to the photon absorption $\Delta n_{ph,abs}$ in the considered excitation interval of CaRh in the light-adapted state.

The increment of absorbed excitation photons $\Delta n_{ph,abs}$ in the considered time increments δt_{exc} is

$$\Delta n_{ph,abs} = \frac{I_{exc} \delta t_{exc}}{h\nu_{exc}} \left[1 - \exp(-\bar{\alpha}_{a,exc,la} l_{exc}) \right] \quad (S8a)$$

where $\bar{\alpha}_{a,exc,la}$ is the absorption coefficient of the light-adapted sample (Rh-527 is absorbing) averaged over the spectral distribution of the excitation light source $g_{LED,i}$ and averaged over excitation time interval δt_{exc} , i.e.,

$$\bar{\alpha}_{a,exc,la} = \frac{\int \alpha_{a, \text{at } \delta t_{exc}/2}(\lambda) g_{LED,i}(\lambda) d\lambda}{\int g_{LED,i}(\lambda) d\lambda} \quad (S8b)$$

S7. Determination of photocycle parameters

The limiting fraction κ_{la1} of excited CaRh_{da}^* converted to CaRh_{la1} at high excitation intensity is obtained from the ratio of the absorption coefficient strength of the S_0 - S_1 transition of CaRh_{la1} at high excitation intensity (dashed curves in Figure 7 for $t_{exc} = 3$ s) to the initial absorption coefficient strength of the S_0 - S_1 transition of CaRh_{da} before excitation (solid curves in Figure 7). That is

$$\kappa_{la1} \approx \frac{\int_{S_0-S_1} \frac{\alpha_{a,\text{CaRh}_{la1}}(\lambda, I_{exc} \rightarrow \infty)}{\lambda} d\lambda}{\int_{S_0-S_1} \frac{\alpha_{a,\text{CaRh}_{da}}(\lambda, I_{exc} = 0)}{\lambda} d\lambda}. \quad (\text{S9})$$

(S_0 - S_1 upper wavelength position in the integration is set to $\lambda_{upper \text{ limit}} = 430$ nm). Thereby it is assumed that the absorption cross-section strengths of the S_0 - S_1 transition of CaRh_{da} and CaRh_{la1} are approximately equal. The analysis gives $\kappa_{la1} \approx 0.73$ for $\lambda_{exc} = 530$ nm, 590 nm, and 470 nm. The limiting fraction κ_{la2} of excited CaRh_{da}^* converted to CaRh_{la2} is $\kappa_{la2} = 1 - \kappa_{la1} \approx 0.27$ for $\lambda_{exc} = 530$ nm, 590 nm, and 470 nm.

Considering the photocycle scheme of Figure 13a and the reaction coordinate scheme of Figure S5 the ratio of $\kappa_{la2}/\kappa_{la1}$ is given by

$$\frac{\kappa_{la2}}{\kappa_{la1}} = \frac{\phi_{cis} \tau_{rec,la2}}{\phi_{trans} \tau_{rec,la1}} = \frac{\phi_{cis} \tau_{rec,la2}}{(1 - \phi_{cis}) \tau_{rec,la1}}. \quad (\text{S10})$$

The κ_{la2} and κ_{la1} values obtained from Equation (S9) give $\kappa_{la2}/\kappa_{la1} \approx 0.37$. Application of Equation (S10) gives $\kappa_{la2}/\kappa_{la1} = 0.37 \pm 0.13$ using $\phi_{cis} = 0.46 \pm 0.05$, $\tau_{rec,la2} = 0.35 \pm 0.01$ s and $\tau_{rec,la1} = 0.8 \pm 0.06$ s.

The absorption coefficient spectrum of $\alpha_a(\lambda, t_{exc} = 3$ s, $\lambda_{exc} = 530$ nm, $I_{exc} = 226$ mW cm⁻²) of Figure 7a is approximately separated in the absorption coefficient contributions $\alpha_{a,\text{CaRh}_{la1}}(\lambda)$ and $\alpha_{a,\text{CaRh}_{la2}}(\lambda)$ which are shown by the thick dashed and the thick dotted curves in Figure 7a (shape of $\alpha_{a,\text{CaRh}_{la2}}(\lambda)$ is taken from initial photo-degradation development of Figure 10). The absorption cross-section spectra of CaRh_{la1} and CaRh_{la2} are given by $\sigma_{a,\text{CaRh}_{la1}}(\lambda) = \alpha_{a,\text{CaRh}_{la1}}(\lambda) / N_{\text{CaRh}_{la1}}$ and $\sigma_{a,\text{CaRh}_{la2}}(\lambda) = \alpha_{a,\text{CaRh}_{la2}}(\lambda) / N_{\text{CaRh}_{la2}}$. The number density of CaRh_{la1} is given by $N_{\text{CaRh}_{la1}} = N_{\text{CaRh},0} \kappa_{la1} \approx 3.66 \times 10^{16}$ cm⁻³, and the number density of CaRh_{la2} is given by $N_{\text{CaRh}_{la2}} = N_{\text{CaRh},0} \kappa_{la2} \approx 1.35 \times 10^{16}$ cm⁻³ ($N_{\text{CaRh},0} = \alpha_a(541 \text{ nm}, t_{exc} = 0) / \sigma_{a,\text{CaRh}_{da}}(541 \text{ nm}) \approx 5.01 \times 10^{16}$ cm⁻³ with $\alpha_a(541 \text{ nm}, t_{exc} = 0) = 8.4$ cm⁻¹ of Figure 7a, $\sigma_{a,\text{CaRh}_{da}}(541 \text{ nm}) = 1.675 \times 10^{-16}$ cm², see top part of Figure S2). The obtained approximate absorption cross-section spectra of CaRh_{la1} and CaRh_{la2} are shown in the bottom part of Figure S2.

The initial quantum yield of all-*trans* – 13-*cis* photo-isomerization ϕ_{cis} (Figure S5) of CaRh_{da} is deduced from the initial light induced absorption change at $\lambda_{pr} = 550$ nm of middle part of Figure 8a for $\lambda_{exc} = 590$ nm and $t_{exc} = 0.0125$ s. ϕ_{cis} is approximately given by

$$\phi_{cis} = \frac{\Delta N_{da}}{\Delta n_{ph,abs}}, \quad (\text{S11})$$

where ΔN_{da} is the increment of length-integrated number density of all-*trans* – 13-*cis* isomerized initially dark-adapted CaRh , and $\Delta n_{ph,abs}$ is the increment of absorbed excitation photons by initially dark-adapted CaRh (Rh-541).

ΔN_{da} is given by

$$\Delta N_{da} = N_{da} l_{exc} \frac{\Delta \alpha_a(\lambda_{pr})}{\alpha_a(\lambda_{pr})} = \frac{\alpha_a(\lambda_{pr})}{\sigma_{a,da}(\lambda_{pr})} l_{exc} \frac{\Delta \alpha_a(\lambda_{pr})}{\alpha_a(\lambda_{pr})} = l_{exc} \frac{\Delta \alpha_a(\lambda_{pr})}{\sigma_{a,da}(\lambda_{pr})} \quad (S12)$$

$N_{da} = \alpha_a(\lambda_{pr}) / \sigma_{a,da}(\lambda_{pr})$ is the number density of CaRh in the dark-adapted state. $\alpha_a(\lambda_{pr})$ is the absorption coefficient of dark-adapted CaRh at λ_{pr} (here used $\lambda_{pr} = 550$ nm). l_{exc} is the sample length in excitation direction (here $l_{exc} = 0.15$ cm), $\Delta \alpha_a(\lambda_{pr})$ is the absorption coefficient change of dark-adapted CaRh at the probe wavelength λ_{pr} due to the photon absorption $\Delta n_{ph,abs}$ within $t_{exc} = 0.0125$ s.

The increment of absorbed excitation photons $\Delta n_{ph,abs}$ in the considered time increment t_{exc} is

$$\Delta n_{ph,abs} = \frac{I_{exc} t_{exc}}{h\nu_{exc}} \left[1 - \exp\left(-\bar{\alpha}_{a,da}(\lambda_{exc}) l_{exc}\right) \right], \quad (S13a)$$

where $\bar{\alpha}_{a,da}(\lambda_{exc})$ is the absorption coefficient of the dark-adapted sample averaged over the spectral distribution of the excitation light source $g_{LED590nm}$, i.e.,

$$\bar{\alpha}_{a,da}(\lambda_{exc}) = \frac{\int \alpha_{a,da}(\lambda) g_{LED590nm}(\lambda) d\lambda}{\int g_{LED590nm}(\lambda) d\lambda}. \quad (S13b)$$

The obtained quantum yield is $\phi_{cis} = 0.46 \pm 0.05$. The quantum yield of all-*trans* back-isomerization is $\phi_{trans} = 1 - \phi_{cis} = 0.54 \pm 0.05$.

S8. Schematic Reaction Coordinate Diagrams for Primary and Secondary Photo-Isomerization Cycles of CaRh

A schematic reaction coordinate diagram for the primary photo-isomerization and deprotonation/re-protonation cycle together with the back-*trans* isomerization with protein restructuring of initially dark-adapted CaRh is shown in Figure S5. The reaction coordinate resembles the dihedral angle of the C13=C14 bond of retinal [8,9]. In Figure S6 a schematic reaction coordinate diagram for the secondary photo-isomerization cycle of light-adapted CaRh_{la1} (PRSB_{all-trans,la1}) is depicted.

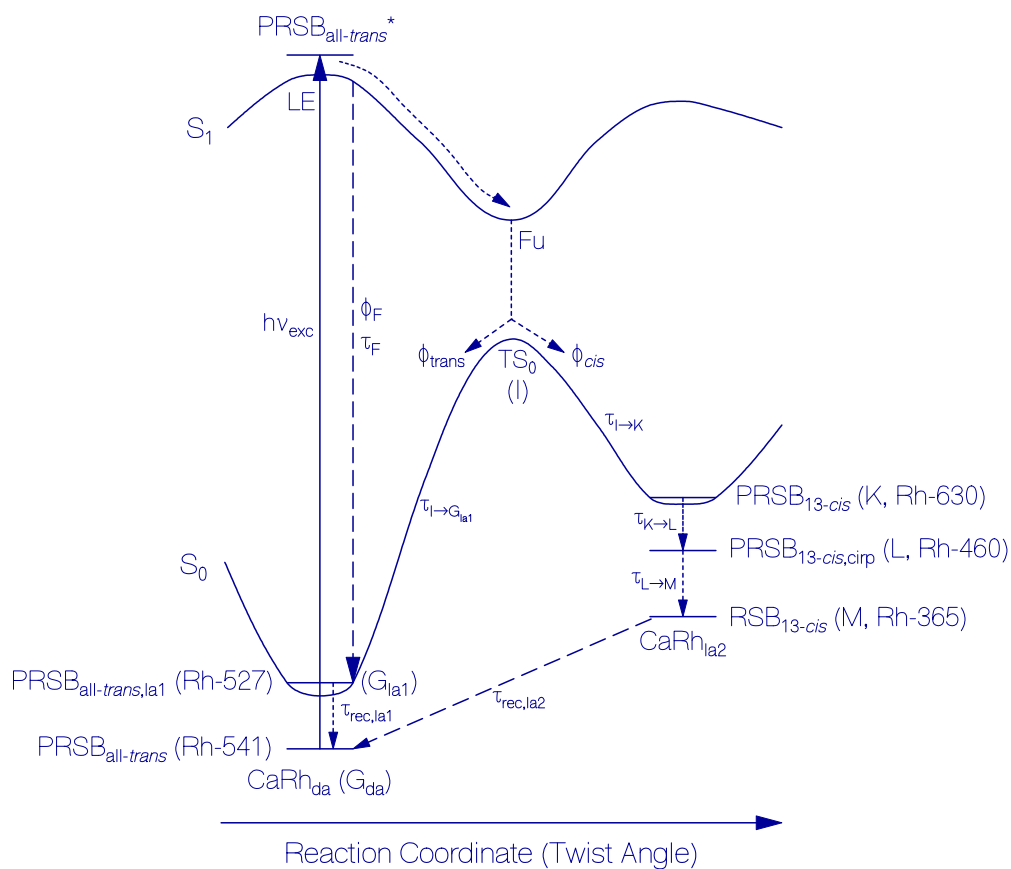


Figure S5. Schematic reaction coordinate diagram for primary photocycle of CaRh in pH 7.3 HEPES/MOPS buffer.

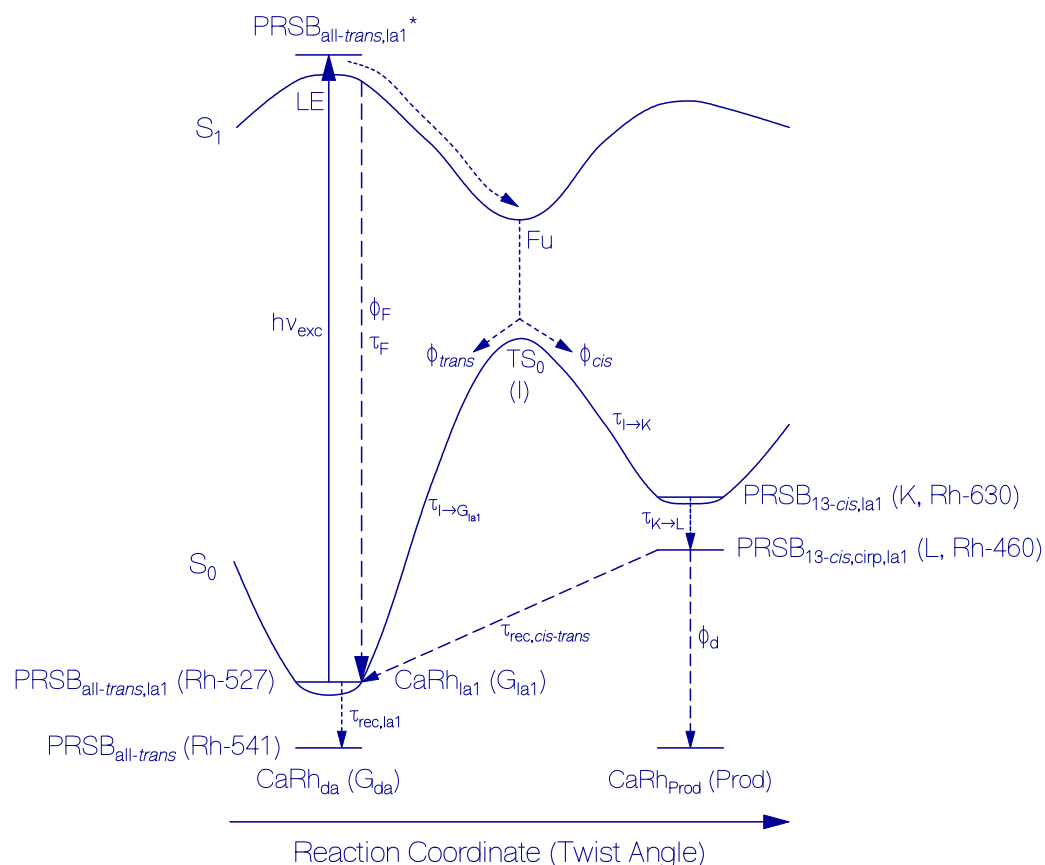


Figure S6. Schematic reaction coordinate diagram for secondary photocycle of CaRh in pH 7.3 HEPES/MOPS buffer.

References

- S1. Honig, B.; Dinur, U.; Birge, R.R.; Ebrey, T.G. The isomer dependence of oscillator strengths in retinal and related molecules. Spectroscopic assignments. *J. Am. Chem. Soc.* **1980**, *102*, 488–494.
- S2. Penzkofer, A.; Stierl, M.; Hegemann, P.; Kateriya, S. Absorption and fluorescence characteristics of photo-activated adenylate cyclase nano-clusters from the amoebflagellate *Nagleria gruberi* NEG-M strain. *Chem. Phys.* **2012**, *392*, 46–54.
- S3. Fischer, H.; Polikarpov, I.; Craievich, A. Average protein density is a molecular-weight-dependent function. *Protein Sci.* **2004**, *13*, 825–828.
- S4. Barer, R.; Tkaczyk, S. Refractive index of concentrated protein solutions. *Nature* **1954**, *173*, 821–822.
- S5. Penzkofer, A.; Stierl, M.; Mathes, T.; Hegemann, P. Absorption and emission spectroscopic characterization of photo-dynamics of photoactivated adenylyl cyclase mutant bPAC-Y7F of *Beggiatoa* sp. *J. Photochem. Photobiol. B Biol.* **2014**, *140*, 182–193.